

Supplementary Information

Hemicellulose content affects the properties of cellulose nanofibrils produced from softwood pulp fibres by LPMO

Salla Koskela,^{a,b} Li Zha,^a Shennan Wang,^a Max Yan,^c and Qi Zhou^{a,b*}

^a Division of Glycoscience, Department of Chemistry, School of Engineering Sciences in
Chemistry, Biotechnology and Health, KTH Royal Institute of Technology, AlbaNova
University Centre, SE-106 91 Stockholm, Sweden

^b Wallenberg Wood Science Center, Department of Fibre and Polymer Technology, KTH
Royal Institute of Technology, SE-100 44 Stockholm, Sweden

^c Department of Applied Physics, KTH Royal Institute of Technology, SE-114 19 Stockholm,
Sweden

Corresponding Author: Q. Zhou, E-mail: qi@kth.se

This Supplementary Information includes:

Table S1 Chemical compositions

Table S2 Physical and mechanical properties of the nanopapers

Figure S1 SDS-PAGE and Western blot analyses

Figure S2 FTIR spectra

Figure S3 XRD patterns

Figure S4 Histogram of width distribution

Figure S5 Loss moduli at pH 8 and pH 2

Table S1. Chemical compositions of starting material pulp fibres and corresponding *Ti*LPMO9E-oxidised CNFs.

Material	Arabinose (%)	Galactose (%)	Glucose (%)	Mannose (%)	Xylose (%)	Glucomannan (%)	Xylan (%)	Total hemicellulose (%)	Cellulose (%)	Klason lignin (%)
Dissolving pulp	0.0	0.0	91.8	1.9	1.6	2.5	1.7	4.2	91.2	3.1
Kraft pulp	0.1	0.0	79.4	8.1	5.1	10.8	5.2	16.0	76.7	3.6
Dissolving CNFs	0.0	0.0	82.8	1.7	1.5	2.3	1.6	3.9	82.2	n/a
Kraft CNFs	0.0	0.0	70.6	7.7	4.6	10.2	4.6	14.8	68.1	n/a

Table S2. Physical and average mechanical properties of nanopapers prepared from *Ti*LPMO9E-oxidised dissolving and kraft CNFs.^a

Material	Porosity (%)	Density (g/cm ³)	Young's modulus (GPa)	Tensile strength (MPa)	Strain-to-failure (%)	Work of fracture (MJ/m ³)
Dissolving CNFs	12.9	1.31	11.1 (0.4)	138 (8)	5.3 (0.2)	5.1 (0.4)
Kraft CNFs	5.5	1.42	16.9 (0.6)	260 (13)	6.3 (0.5)	10.6 (1.4)

^a The values in parentheses represent standard deviation of four technical replicates.

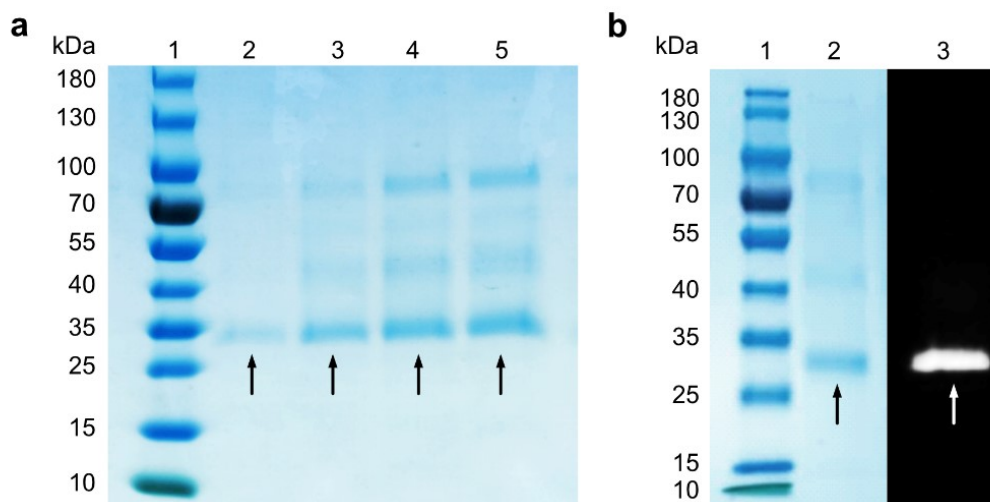


Figure S1. Production of *T. terrestris* TtLPMO9E in *P. pastoris*. (a) SDS-PAGE where lane 1 shows a size marker protein ladder, and lanes 2–5 contain *P. pastoris* culture supernatant from 1 to 4 days of methanol induction. (b) SDS-PAGE and Western blot analyses of purified TtLPMO9E. Lane 1 shows a size marker protein ladder, and lanes 2 and 3 contain the LPMO. The bands indicated by arrows correspond to the heterologously expressed enzyme.

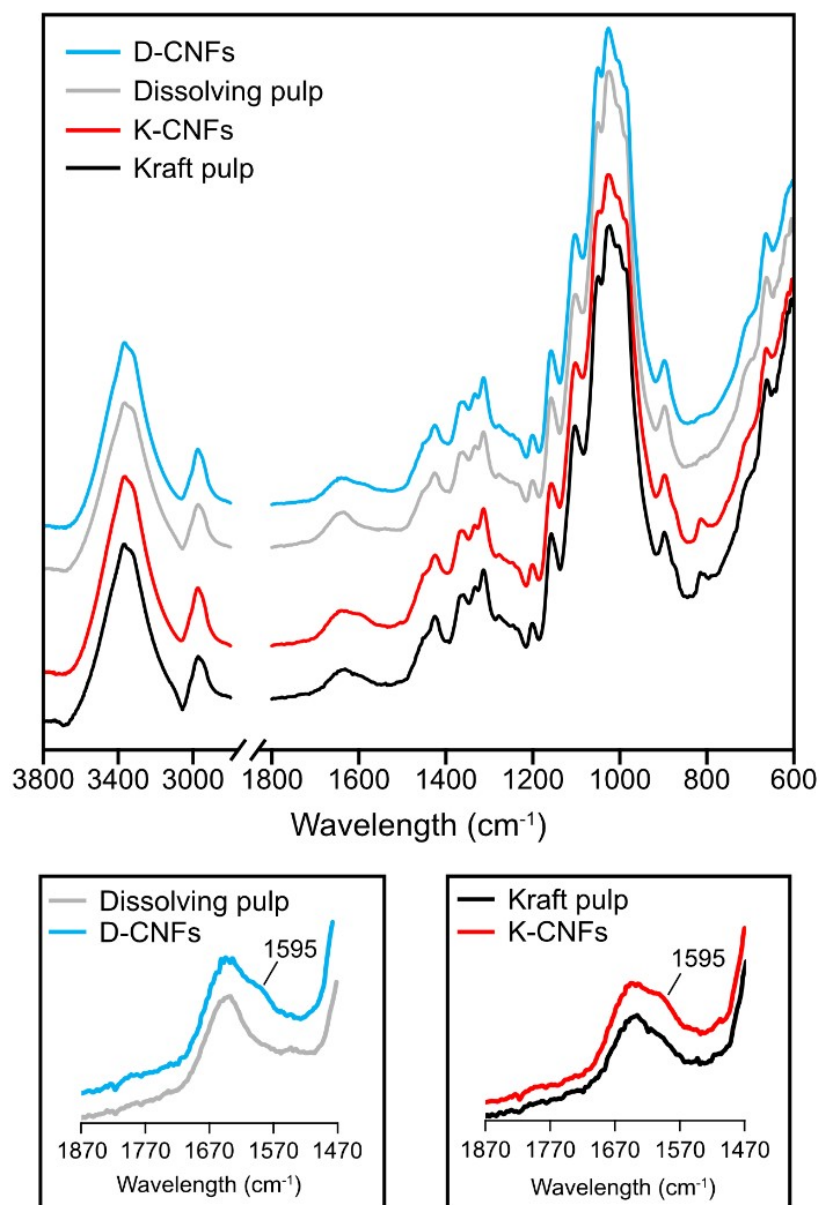


Figure S2. FTIR spectra of D-CNFs and K-CNFs, as compared to the starting dissolving pulp and kraft pulp fibres. The peak appeared at 1595 cm⁻¹ in the *Ti*LPMO9E-oxidised samples corresponds to the carboxylate –COONa. The spectra have been normalised at 1028 cm⁻¹, which corresponds to the pyranose ring ether vibration of cellulose.

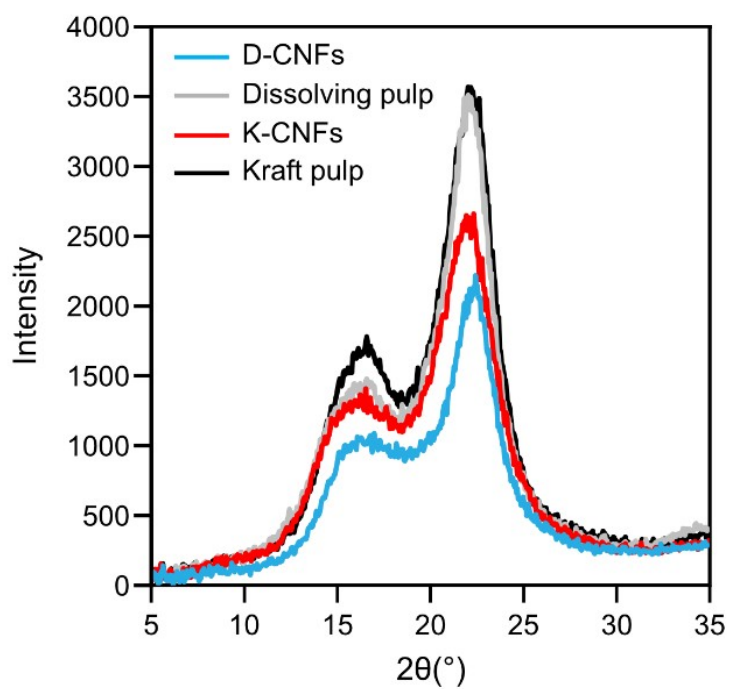


Figure S3. XRD patterns of D-CNFs and K-CNFs, as compared to the starting dissolving pulp and kraft pulp fibres.

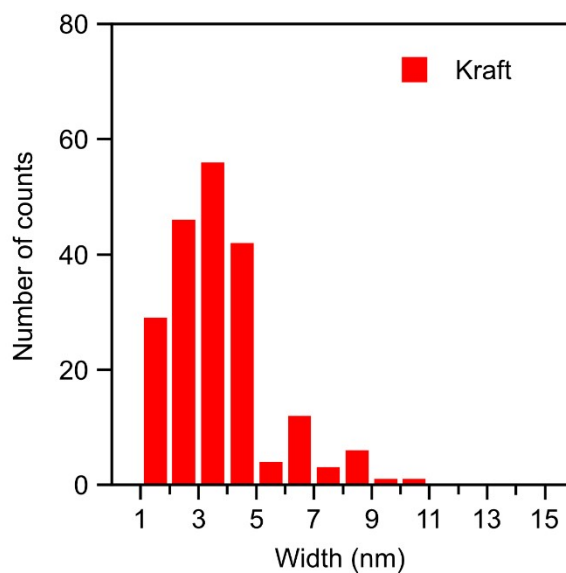


Figure S4. Histogram for the width distribution of K-CNFs. The histogram was obtained from the AFM images.

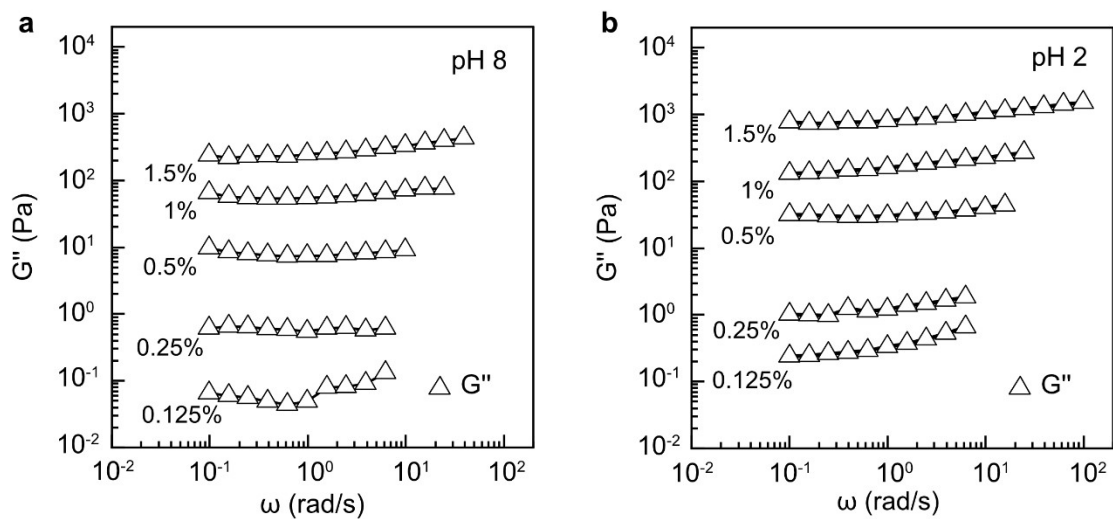


Figure S5. The loss moduli (G'') of the *TtLPMO9E*-oxidised K-CNFs suspensions. The loss modulus (G'') is presented as a function of frequency. The measurements were conducted at 25 °C in (a) aqueous dispersion at pH 8, and (b) after cross-linking into hydrogels at pH 2.